

Electron localization into spin-polaron state in MnSi

Vyacheslav G. Storchak,^{1,*} Jess H. Brewer,² Roger L. Lichti,³ Thomas A. Lograsso,⁴ and Deborah L. Schlage⁴

¹Russian Research Centre “Kurchatov Institute,” Kurchatov Sq. 1, Moscow 123182, Russia

²Department of Physics and Astronomy, University of British Columbia, Vancouver, BC, Canada V6T 1Z1

³Department of Physics, Texas Tech University, Lubbock, Texas 79409, USA

⁴Ames Laboratory, Iowa State University, Ames, Iowa 50011, USA

(Received 15 March 2011; published 13 April 2011)

Strong electron localization into a bound state has been found in both paramagnetic and ferromagnetic states of the transition metal compound MnSi by muon spin-rotation spectroscopy in magnetic fields up to 7 T and from 2 K to room temperature. This bound state, with a characteristic radius $R \approx 0.4$ nm and net spin $S = 24 \pm 2$, is consistent with confinement of the electron’s wave function within roughly one lattice cell of MnSi and is suggested to be a spin polaron. Such spin polarons may form due to a strong exchange interaction between itinerant electrons and the magnetic electrons of Mn ions of the same $3d$ type; as such, they might affect the peculiar electronic and magnetic properties of MnSi.

DOI: 10.1103/PhysRevB.83.140404

PACS number(s): 76.75.+i, 71.70.Gm, 72.80.Ga, 74.20.Mn

The transport properties of transition metal compounds near a crossover from localized to itinerant electron behavior present formidable challenges to theoretical explication, including non-Fermi-liquid (NFL) behavior when the interaction energies of the electrons are comparable to their kinetic energies.^{1,2} The specific quantum states that might replace the Fermi liquid remain unclear.³ It has long been recognized that the d electrons responsible for magnetism in transition metals have a dual nature; in their ground state, the itinerant electrons are described by band theory, while at elevated temperature, they exhibit properties characteristic of a system of local moments.^{4,5} In magnetic systems that occupy the borderline between these two extremes, the so-called “nearly ferromagnetic metals,” NFL behavior is often found in the phase diagram near a magnetically ordered phase, indicating that the NFL state may be linked to magnetic instabilities.^{1,2} The best-known examples include ZrZn₂,^{3,6} Ni₃Al,⁷ Pd alloys,⁸ UGe₂,⁹ and MnSi.^{10–12}

The latter, MnSi, represents the canonical borderline case of a weak itinerant ferromagnet in the evolution of metallic ferromagnetism away from the localized moment extreme of ferromagnetic (FM) Fe (with well-defined local magnetic moments) toward the correlated paramagnet Pd. Under ambient conditions, MnSi orders below $T_c = 29.5$ K into a helimagnetic phase with a rather long period of 18 nm along the 111 direction of the noncentrosymmetric cubic B20 crystal structure.¹³ An applied magnetic field $\gtrsim 0.1$ T unpins the helical order to align the resulting conical phase along the field; magnetic fields exceeding 0.6 T establish a spin-aligned FM state, which completes the phase diagram at ambient pressure.¹⁴ Above T_c , MnSi exhibits a Curie-Weiss-type susceptibility with an effective paramagnetic (PM) moment $m_{\text{PM}} = 2.2\mu_B$ per Mn, while its spontaneous magnetic moment in the FM phase is significantly smaller: $m_{\text{FM}} = 0.4\mu_B$ per Mn. Although such an enhanced ratio of m_{PM} to m_{FM} may be accounted for by self-consistent renormalization (SCR) within the enhanced spin-fluctuation approach,^{4,5} *ab initio* calculations predict a significantly higher $m_{\text{FM}} \approx 1\mu_B$.^{15,16} Accordingly, recent ²⁹Si NMR (Ref. 16) and μ SR (Ref. 17)

studies have questioned the validity of the SCR model as applied to MnSi.

Most recently, a number of unanticipated effects have been discovered in MnSi: the electrical resistivity at low temperature changes abruptly from the standard FL T^2 behavior to $T^{3/2}$,^{11,12} while the conventional long-range FM state is suppressed to give way to a phase with “partial magnetic order” at a hydrostatic pressure $p_c = 14.6$ kbar.¹⁸ These observations contradict the predictions of the FL theory and require explanation. Furthermore, infrared optical conductivity and de Haas–van Alphen experiments indicate strong electron scattering above ~ 200 K, while at low temperature, the electron effective mass m^* is dramatically enhanced (up to $17m_e$).^{19,20} All these effects suggest strong coupling to spin fluctuations, the nature of which remains unclear.

The observation of partial magnetic order raises the question of spatial homogeneity of the underlying spin structure in MnSi.¹⁴ Inhomogeneous magnetism in MnSi is found at high pressure by neutron scattering,¹⁸ zero-field ²⁹Si NMR,²¹ and μ SR.²² The length scale of such magnetic inhomogeneities is, however, not identified. On the other hand, resistivity¹⁰ and optical conductivity¹⁹ measurements show anomalously enhanced quasiparticle-quasiparticle scattering cross sections consistent with inhomogeneities on a scale of the order of the lattice spacing. The origin of such magnetic inhomogeneities needs to be identified.

In MnSi, all these unusual properties indicate strong $3d$ electron correlations. In fact, the entire family of B20 isostructural transition metal monosilicides exhibits discontinuous evolution of electronic and magnetic properties upon doping, from the $3d^5$ itinerant FM metal MnSi to the $3d^6$ paramagnetic semiconductor FeSi to the $3d^7$ diamagnetic metal CoSi.²³ MnSi, FeSi, and CoSi form an isostructural dilution series of ternary and quaternary strongly correlated compounds, which not only permits conversion of a semiconductor into an unconventional metal, but also exhibits NFL behavior.²⁴ Such unusual electronic properties are accompanied by the emerging physics of skyrmions,^{25–27} which clearly indicates microscopic magnetic inhomogeneities.

In this Rapid Communication, we present spectroscopic evidence for electron confinement in MnSi into a bound state that we believe is a spin polaron, which can result in both microscopic magnetic inhomogeneities and an effective-mass enhancement with possible NFL behavior.

A hierarchy of three well-separated energy and length scales is generally thought to determine the magnetic and electronic properties of MnSi (Ref. 18): (1) an exchange interaction that causes FM over a length scale of many lattice spacings; (2) the weak spin-orbit interaction that produces helical modulation with a long wavelength (~ 18 nm at ambient pressure); and (3) a still weaker crystal anisotropy term that locks the direction of the spiral on a length scale of 1000 nm within a single domain. In strongly correlated electron systems, however, one must also take into account the much stronger exchange interaction J between itinerant carriers and localized spins, which is typically confined to within one lattice spacing. In treating this interaction, two limiting cases are important: (a) when the itinerant electron bandwidth W is large compared with J and (b) the opposite limit, when $J \gg W$. The former applies to the s - f exchange in rare-earth compounds where the extremely localized f electrons are screened by other shells. The opposite extreme ($W \ll J$) provides the basis for the well-known double exchange in transition metal compounds. As odd as it may seem, this inequality is likely to be quite realistic in such compounds, where the charge carriers are often of the same d type as the localized spins.^{28–30} MnSi falls into an intermediate regime $J/W \sim 1$: the width of its $3d$ band is $W \approx 2$ eV,^{15,31} while $J \approx 0.6$ eV.²⁰ Both *ab initio* calculations¹⁵ and recent measurements³² show that the large density of Mn $3d$ states within the $3d$ band(s) falls at the Fermi level, ensuring a strong exchange interaction between itinerant carriers and local spins of the same d type in MnSi.

Such an exchange interaction can dramatically modify the electron state *via* its localization into a *spin polaron* (SP).³³ The SP is a few-body state formed by an electron that mediates a FM interaction between magnetic ions in its immediate environment, the direct coupling of which is rather weak. In such a system, an electron's energy depends strongly on the magnetization, with the minimum energy being achieved by FM ordering²⁸: the electron will then localize and form a FM “droplet” over the extent of its wave function in a host of any other state (in particular, PM or helimagnetic). The electron coupled to its immediate FM environment behaves as a single entity with a giant spin S , i.e., a spin polaron. In the process of electron localization, the exchange interaction is opposed by the increase of the electron kinetic energy and the entropy term due to ordering within the polaron, so the net change in the free energy

$$\Delta F = \frac{\hbar^2}{2m^*R^2} + T\Delta S - J\frac{a^3}{R^3} \quad (1)$$

has a minimum as a function of R , the radius of the electron confinement; ΔF decreases with decreasing R until $R \ll a$ (the lattice constant), at which point the electron wave function no longer overlaps even the nearest ions, and the exchange term vanishes.²⁸ At low temperature, the entropy term $T\Delta S$ is small; each of the remaining two terms in Eq. (1) is of the order of electronvolts and far exceeds any other energy scale in the problem.

The Coulomb interaction, which is important in magnetic semiconductors (MS),^{34,35} is effectively screened in metals. In MnSi, the high electron concentration ($\sim 4-8 \times 10^{22}$ cm⁻³) (Ref. 36) ensures that the long-range Coulomb term is screened over distances $\gtrsim 0.1$ nm. Then, J reduces the length scale of the electron confinement to the order of one unit cell.^{29,30,34,35,37}

Assorted SP have recently been detected in $3d$ and $4f$ MS (Refs. 29, 34, and 35) and in the $5d$ correlated metal Cd₂Re₂O₇ (Ref. 30) *via* positive muon spin-rotation (μ^+ SR) spectroscopy,³⁸ analogous to earlier studies of nonmagnetic semiconductors,³⁹ which revealed the details of electron capture to form the muonium ($\text{Mu} \equiv \mu^+e^-$) atom (a light analog of the H atom).⁴⁰

Single crystals of MnSi for the current studies were grown from a stoichiometric melt. X-ray studies at 300 K reveal a lattice parameter $a = 0.4559(1)$ nm and mosaicity less than 0.2° . The residual resistivity of each sample was less than $2 \mu\Omega\text{cm}$. SQUID measurements yield effective moments consistent with literature values in both PM and FM phases.

Time-differential μ^+ SR experiments³⁸ using 100% spin-polarized positive muons implanted into these samples were carried out on the M15 muon channel at TRIUMF using the *HiTime* spectrometer. In such experiments, the time interval between a muon stopping in the sample and the subsequent detection of its decay positron in one of four detectors is digitized, and the corresponding bin of a time histogram is incremented. After $\sim 10^7$ such events, the four histograms show the probability of a positron being emitted in the $\pm\hat{x}$ or $\pm\hat{y}$ directions as a function of time. In a magnetic field $\vec{B} = B\hat{z}$ transverse to the initial muon spin direction, these four histograms can be combined³⁸ into a complex “asymmetry” time spectrum, which can be transformed into a rotating reference frame for display (as in the inset of Fig. 1) or Fourier transformed (Figs. 1 and 2) to reveal the μ^+ SR frequency spectrum.

Fourier transforms of the μ^+ SR time spectra exhibit two peaks (Fig. 1) shifted to lower frequencies relative to

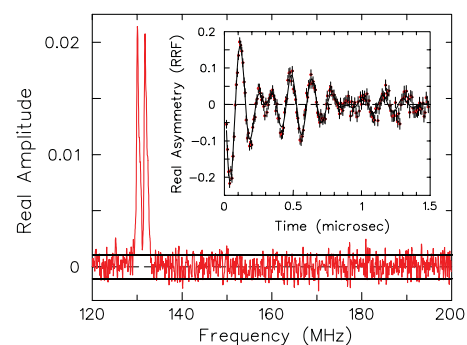


FIG. 1. (Color online) Frequency spectrum of muon spin precession in MnSi in a transverse magnetic field of $B = 1$ T at $T = 50$ K. The unitless vertical axis is the real part of the Fourier transform of the inset time spectrum. The two-frequency precession is characteristic of a localized electron hyperfine-coupled to a muon. Inset: muon decay asymmetry data (circles) and uncertainties (vertical bars) as a function of time since the muon's arrival, displayed in a rotating reference frame at 135 MHz, from which the frequency spectrum is obtained by a fast Fourier transform. The solid black line is a χ^2 -minimization fit to the data.

the reference frequency $\nu_\mu = \gamma_\mu B/2\pi$ (where $\gamma_\mu = 2\pi \times 135.53879$ MHz/T is the muon gyromagnetic ratio and B is the magnetic field). There is essentially no background signal in our MnSi spectra.

The two lines shown in Fig. 1 constitute the characteristic signature of a coupled μ^+e^- spin system in high field.^{29,30,34,35,38,39} For such a system, these signals correspond to two muon spin-flip transitions between states with fixed electron spin orientation, the splitting between them being determined by the muon-electron hyperfine interaction A .³⁴ In a metal, the Coulomb interaction is screened, so electrostatically bound Mu can not form; thus, the conventional interpretation of multiple signals in magnetic metals is that bare muons stop in several magnetically inequivalent lattice sites. However, in the PM phase, fast spin fluctuations reduce any local fields at such sites to an average Knight shift, which is typically 2 to 3 orders of magnitude less than the observed splittings.^{29,30,34,35} The fact that the splittings do not change abruptly at T_c rules out this conventional interpretation. Moreover, observation of a unique level-crossing resonance⁴¹ confirms a *single* stopping site for the muon in MnSi.

Two-frequency Mu-like spectra are found throughout the temperature range 2–305 K in magnetic fields 0.25–7 T. We argue that the observed bound state is a spin polaron: In a PM and/or metallic environment, the strong pair exchange interaction of the Mu electron with the itinerant spins (spin exchange³⁹) would result in rapid spin fluctuations of the Mu electron, averaging the hyperfine interaction to zero if *local* ferromagnetic ordering mediated by the aforementioned electron did not hold said electron's spin "fixed".^{30,34} The mere observation of Mu-like lines in the μ^+ SR spectra of a magnetically disordered metal is strong evidence for SP formation.³⁰ However, by no means does application of B cause formation of a SP, as the relevant energy scale is at least 2 orders of magnitude less than the energies involved in its formation [see Eq. (1)]. The evolution of SP signals with temperature is presented in Fig. 2. The shift of the centroid

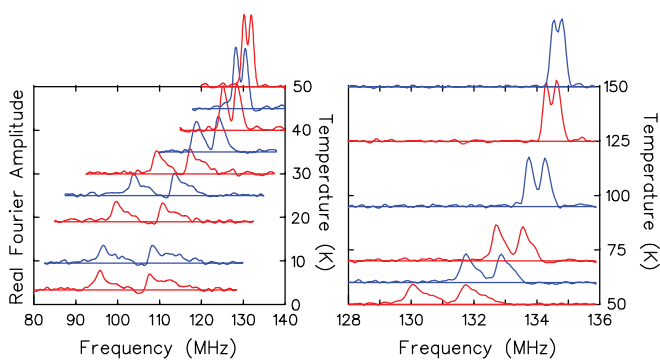


FIG. 2. (Color online) Fourier transforms of the muon spin precession signal in MnSi in a transverse external magnetic field of 1 T at different temperatures. Characteristic SP lines persist through the FM transition down to the lowest measured temperature. Note the frequency scale change between low and high T , reflecting the dramatic reduction of the splitting at high T . The Fourier transforms are taken over the first $1\mu\text{s}$ of the time spectra for the low- T data and over the first $6\mu\text{s}$ for the high- T data, due to the faster relaxation rate in the former. The 50-K time spectrum is analyzed both ways; its 6- μs version gives the same frequency spectrum shown in Fig. 1.

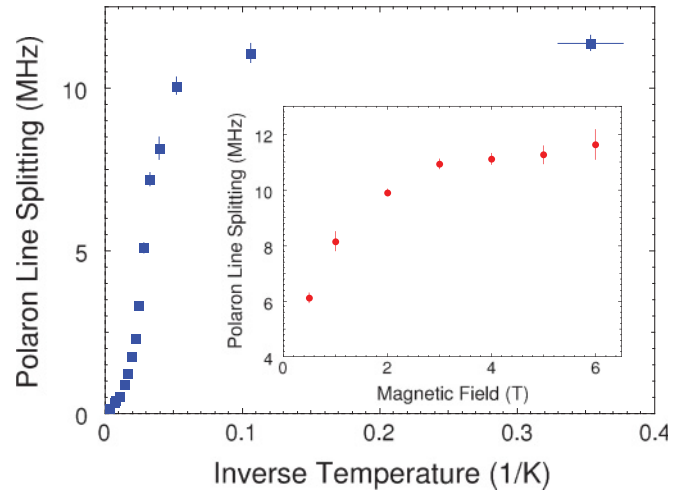


FIG. 3. (Color online) Temperature dependence of the SP frequency splitting $\Delta\nu$ in MnSi in a magnetic field of $B = 1$ T. Inset: magnetic field dependence of $\Delta\nu$ at $T = 25$ K. Both curves saturate at the same value of $A = 11.5 \pm 1$ MHz.

of the two-line SP spectra scales with the bulk susceptibility, similar to corresponding shifts in $3d$ and $4f$ MS.^{29,34,35} At all T below ~ 75 K, hints of structure appear in both peaks of the Fourier spectra, suggesting possible effects of crystalline anisotropies.³⁰ However, rapid muon spin relaxation precludes resolution of any possible additional lines.

The SP line splitting $\Delta\nu$ reveals the characteristic size and the composite spin \mathcal{S} of the SP through the hyperfine coupling A .³⁴ For $g\mu_B B \ll k_B T$, $\Delta\nu$ is a linear function of both B and $1/T$ (Ref. 34):

$$\Delta\nu = A \left(\frac{g\mu_B B}{3k_B T} \right) (\mathcal{S} + 1). \quad (2)$$

At low T and high B , however, \mathcal{S} is fully polarized and $\Delta\nu$ saturates at a value of A .^{34,38} In MnSi, the splitting $\Delta\nu$ saturates as a function of both $1/T$ (in a magnetic field $B = 1$ T) and B (at $T = 25$ K) at the same value $A = 12 \pm 1$ MHz (Fig. 3). For a $1s$ Mu atom, the value of A scales as $A_{\text{vac}}(a_0/R)^3$, where $A_{\text{vac}} = 4463$ MHz is the hyperfine frequency of Mu in vacuum with $R = a_0 = 0.0529$ nm and R is the atom's characteristic Bohr radius. We thus find $R \approx 0.4$ nm, corresponding to electron confinement within one unit cell of MnSi, which contains four Mn ions with spin-5/2 each. When fully polarized, such a SP has $\mathcal{S} = 10.5$ (four Mn ions plus the localized electron). The value of \mathcal{S} extracted from the slope of the linear dependence of $\Delta\nu$ on $1/T$ (Ref. 34) in the 40–300 K range amounts to $\mathcal{S} = 24 \pm 2$, reasonably consistent with a fully polarized core of four Mn ions plus an unsaturated halo similar to that in MS.^{29,34,35}

As the exchange term J is the dominant interaction leading to SP formation (the Coulomb interaction is effectively screened), the role of the muon is reduced to that of an "innocent observer": we suggest that the host lattice is populated by free SP, one of which is captured by the muon, from which we detect Mu-like spectra characteristic of a bound electron state, as in $\text{Cd}_2\text{Re}_2\text{O}_7$.³⁰

The exchange contribution amounts to the difference between the PM disorder of the host and the enhanced (FM)

order within the SP. In a fully saturated FM state, the exchange contribution to the localization would be negligible, as the lattice spins are already aligned; in FM MnSi, however, the rather low (unsaturated) effective $m_{\text{FM}} = 0.4\mu_B$ does not prevent electron localization, which completes spin alignment within the SP.

In MnSi, the size of such SP coincides with the anomalously enhanced quasiparticle scattering cross sections found by resistivity and optical conductivity, as well as the microscopic magnetic inhomogeneities, both of which are on the order of one unit cell. Accordingly, the spin-glass-like resistivity in the

purest samples¹¹ and the NFL behavior at low temperature are consistent with SP formation.

In general, formation of SP might considerably shape current views on correlated electron materials, including those exhibiting superconductivity.^{30,42}

This work was supported by the NBIC Center of the Kurchatov Institute, NSERC of Canada, and the US DoE (Contracts No. DE-SC0001769, No. DE-AC02-07CH11358, and BES Division of Materials Sciences).

*mussr@triumf.ca

¹G. R. Stewart, *Rev. Mod. Phys.* **73**, 797 (2001).

²S. M. Varma *et al.*, *Phys. Rep.* **361**, 267 (2002).

³R. P. Smith *et al.*, *Nature (London)* **455**, 1220 (2008).

⁴T. Moriya, *Spin Fluctuations in Itinerant Electron Magnetism* (Springer, Berlin, 1985).

⁵G. G. Lonzarich and L. Taillefer, *J. Phys. C: Solid State Phys.* **18**, 4339 (1985).

⁶M. Uhlarz *et al.*, *Phys. Rev. Lett.* **93**, 256404 (2004).

⁷P. G. Niklowitz *et al.*, *Phys. Rev. B* **72**, 024424 (2005).

⁸P. G. Nicklas *et al.*, *Phys. Rev. Lett.* **82**, 4268 (1999).

⁹S. S. Saxena *et al.*, *Nature (London)* **406**, 587 (2000).

¹⁰C. Pfleiderer *et al.*, *Phys. Rev. B* **55**, 8330 (1997).

¹¹C. Pfleiderer *et al.*, *Nature (London)* **414**, 427 (2001).

¹²N. Doiron-Leyraud *et al.*, *Nature (London)* **425**, 595 (2003).

¹³Y. Ishikawa *et al.*, *Phys. Rev. B* **31**, 5884 (1985).

¹⁴C. Pfleiderer *et al.*, *J. Phys. C: Solid State Phys.* **21**, 164215 (2009).

¹⁵T. Jeong and W. E. Pickett, *Phys. Rev. B* **70**, 075114 (2004).

¹⁶M. Corti *et al.*, *Phys. Rev. B* **75**, 115111 (2007).

¹⁷A. Yaouanc *et al.*, *J. Phys. (Moscow)* **17**, L129 (2005).

¹⁸C. Pfleiderer *et al.*, *Nature (London)* **427**, 227 (2004).

¹⁹F. P. Mena *et al.*, *Phys. Rev. B* **67**, 241101(R) (2003).

²⁰L. Taillefer *et al.*, *J. Magn. Magn. Mater.* **54–57**, 957 (1986).

²¹W. Yu *et al.*, *Phys. Rev. Lett.* **92**, 086403 (2004).

²²Y. J. Uemura *et al.*, *Nat. Phys.* **3**, 34 (2007).

²³J. Teyssier *et al.*, *Phys. Rev. B* **82**, 064417 (2010).

²⁴N. Manyala *et al.*, *Nature (London)* **454**, 976 (2008).

²⁵S. Muhlbauer *et al.*, *Science* **323**, 915 (2009).

²⁶X. Z. Yu *et al.*, *Nature (London)* **465**, 901 (2010).

²⁷W. Munzer *et al.*, *Phys. Rev. B* **81**, 041203(R) (2010).

²⁸E. L. Nagaev, *Colossal Magnetoresistance and Phase Separation* (Imperial College Press, London, 2002).

²⁹V. G. Storchak *et al.*, *J. Phys. Condens. Matter* **22**, 495601 (2010).

³⁰V. G. Storchak *et al.*, *Phys. Rev. Lett.* **105**, 076402 (2010).

³¹F. Carbone *et al.*, *Phys. Rev. B* **73**, 085114 (2006).

³²K. Kura *et al.*, *J. Phys. Soc. Jpn.* **77**, 024709 (2008).

³³P. G. de Gennes, *Phys. Rev.* **118**, 141 (1960).

³⁴V. G. Storchak *et al.*, *Phys. Rev. B* **80**, 235203 (2009); **81**, 153201 (2010); **83**, 077202 (2011).

³⁵V. G. Storchak *et al.*, *Phys. Rev. B* **79**, 193205 (2009).

³⁶A. Neubauer *et al.*, *Phys. Rev. Lett.* **102**, 186602 (2009).

³⁷V. G. Storchak *et al.*, *Phys. Rev. B* **79**, 220406(R) (2009).

³⁸J. H. Brewer, *Encyclopedia of Applied Physics*, Vol. 11 (VCH Publishers, New York, 1994), pp. 23–53.

³⁹B. D. Patterson, *Rev. Mod. Phys.* **60**, 69 (1988).

⁴⁰V. G. Storchak *et al.*, *Phys. Rev. Lett.* **78**, 2835 (1997); V. G. Storchak *et al.*, *Phys. Rev. B* **67**, 121201 (2003).

⁴¹R. Kadono *et al.*, *Phys. Rev. B* **48**, 16803 (1993).

⁴²Recently, by using μ^+ SR technique, we found SP in several heavy fermion superconductors and UGe₂.